International Journal of Climatology

International Journal of Climatology | RMetS

RESEARCH ARTICLE OPEN ACCESS

Thermodynamic Differences Between Moderately and Extremely Long Heat Waves in South Korea

Minjeong Cho[1] | Ha-Rim Kim[2,3] | Changhyun Yoo[1] | Yong-Sang Choi[1]

[1]Department of Climate and Energy Systems Engineering, Ewha Womans University, Seoul, South Korea | [2]Center for Climate/Environmental Change Prediction Research, Ewha Womans University, Seoul, South Korea | [3]Supercomputer Center, Institute of Environmental and Marine Science Technology, Pukyong National University, Busan, South Korea

Correspondence: Yong-Sang Choi (ysc@ewha.ac.kr)

Received: 7 June 2025 | **Revised:** 1 October 2025 | **Accepted:** 6 October 2025

Funding: This research was supported by the Specialized University Program of the Korea Meteorological Institute (KMI). This research was also supported by the Basic Science Research Program through the National Research Foundation of Korea (NRF), funded by the Ministry of Education (2018R1A6A1A08025520) and by a National Research Foundation of Korea (NRF) grant funded by the Korean government (MSIT) (2021R1A2C1093402). Minjeong Cho was supported by an Ewha Womans University scholarship in 2022.

Keywords: land–atmosphere interaction | prolonged summer heat wave | South Korea | thermodynamics

ABSTRACT

Heat waves in South Korea have become markedly longer, highlighting a need to better understand the physical mechanisms governing their persistence. Therefore, we first categorised 52 years (1973–2024) of summer heat waves into moderately long events (MLEs; 5–9 days) and extremely long events (ELEs; ≥ 10 days) based on their duration and statistical distribution. Then, we analysed each type of summer heat wave using a stage-based framework that focused on their growth, maintenance and decay stages to examine the thermodynamic evolution of these events. We found that, although both MLEs and ELEs exhibited similar initial warming driven by warm advection and adiabatic heating during the growth stage, ELEs developed distinct thermodynamic features during the maintenance and decay stages. The persistent high-pressure system over South Korea induced pronounced subsidence that sustained adiabatic warming and inhibited cloud formation, enhancing surface downward shortwave radiation and amplifying surface warming. This, in turn, depleted soil moisture, enhancing sensible heat flux through land–atmosphere interactions, thereby strengthening diabatic heating and delaying surface cooling. Those thermodynamic processes sustained ELEs, while large-scale circulation provided a dynamical background for the stagnation of the high-pressure systems. By distinguishing the thermodynamic evolution of ELEs from that of MLEs, this study provides key insights into the mechanisms driving the longer heat waves over South Korea.

1 | Introduction

Extreme heat waves have become more frequent around the world in recent decades (Trenberth and Fasullo 2012; Perkins-Kirkpatrick and Lewis 2020). Notable examples include the summer of 2003 in Europe (Robine et al. 2008; García-Herrera et al. 2010), the summer of 2010 in Russia (Revich and Shaposhnikov 2012; Otto et al. 2012; Seo et al. 2019), the summer of 2018 in East Asia (Iwasaki et al. 2019; Ren et al. 2020) and the summer of 2021 in North America (Thompson et al. 2022). These events posed substantial risks to human health, society, the economy, agriculture and ecosystems (Perkins 2015; Bador et al. 2017; Ho et al. 2020). Numerous studies have noted an increasing trend in the frequency, intensity and persistence of extreme heat waves and those trends are projected to continue worldwide (Rohini et al. 2019; Chen et al. 2021; Ma and Yuan 2021; Allan et al. 2023).

Mirroring the global trend, South Korea has also experienced prolonged and intense heat waves in recent decades (Kysely and Kim 2009; Lee et al. 2020). For instance, a record-breaking heat wave lasting 31.5 days occurred in July–August 2018, when extremely high temperatures had severe socioeconomic effects, including 48 heat-related fatalities (Min, Kim, et al. 2020). Other notable long-lasting heat waves occurred in 1994, 2013 and 2016 (Kim et al. 2008; Kim et al. 2018; Yoon et al. 2018). Although prolonged heat waves intensify cumulative heat stress (Mazdiyasni et al. 2019; De Polt et al. 2023), previous studies have predominantly focused on their frequency and intensity, with comparatively little attention given to their duration. Given the ongoing trend of prolonged heat waves, understanding the mechanisms underlying their extended duration has become increasingly important.

Korean heat waves are generally associated with anticyclonic circulation, which contributes to their onset (Yoon et al. 2021). This circulation induces descending air motion, clear-sky conditions and increased solar radiation, resulting in surface heating (Yeo et al. 2019; Yoon et al. 2018). Choi et al. (2021) highlighted that prolonged heat waves in August resulted from both anticyclones and stagnant weather systems driven by large-scale teleconnections. Furthermore, Yeh et al. (2018) reported that the long-lasting heat wave of 2016 was caused by a persistent high-pressure system over the Kamchatka Peninsula that acted as an atmospheric block downstream on the Korean Peninsula at the same time that an anomalous high over Mongolia induced warm advection into Korea via northerly winds. Min, Chung, et al. (2020) observed that widespread blocking over the North Pacific Ocean and Asia induced stationary weather patterns over South Korea during severe heat waves in 1994, 2013 and 2016. According to Ha et al. (2020), the northwestward expansion of the North Pacific High and its persistence until August contributed to sustained warming over South Korea in 2018. Those studies emphasize the importance of large-scale atmospheric circulation in the persistence of heat waves.

From the perspective of atmospheric circulation, previous studies have linked Korean heat waves to several teleconnection patterns (Lee and Lee 2016; Choi et al. 2020; Lee, Cho, et al. 2024). Among them, the meridionally propagating Rossby waves called the Pacific-Japan (PJ) pattern are regarded as one of the key drivers (Nitta 1987). Noh et al. (2021) demonstrated that the positive phase of the PJ pattern induced warm horizontal advection in the lower troposphere, thereby intensifying heat waves over Korea and Japan. Korea is also influenced by the circumglobal teleconnection (CGT) pattern, a zonally elongated wave train in the mid-latitudes (Ding and Wang 2005). Kim et al. (2019) suggested that diabatic heating in northwestern India can strengthen the CGT pattern, amplifying Korean heat waves. More recently, remote influences from the Arctic have emerged as an important factor affecting summer weather in the mid-latitudes. Notably, the influence of Arctic variability, such as the Arctic Oscillation (AO), has increased through changes in westerly intensity that promote the stagnation of high pressure over East Asia, including South Korea and prolonged heat waves (Lee and Lee 2016; Wu and Francis 2019).

In addition to those anomalous circulations, the evolution of heat waves also depends critically on local processes, such as thermodynamic processes and land–atmosphere coupling (Zhang et al. 2011; Lin et al. 2022; Domeisen et al. 2023; Barriopedro et al. 2023; Chen et al. 2024). Such processes include horizontal advection of air from climatologically warmer regions, adiabatic warming due to subsidence and diabatic heating caused by radiation and surface heat flux. Additionally, local conditions, including reduced cloud cover and soil moisture deficits, can amplify surface heating by altering the surface energy balance (Seneviratne et al. 2010; Wang et al. 2022; Tak et al. 2024; Liu et al. 2025). Although those processes have been studied individually or through case studies, systematic understanding of how thermodynamic factors collectively contribute to the persistence of extreme heat waves, especially those of exceptional duration, remains insufficient.

In this study, we address that gap by examining the thermodynamic characteristics of prolonged heat waves over South Korea, with a particular emphasis on their temporal evolution across the distinct stages of growth, maintenance and decay. We classified heat waves lasting at least 5 days into moderately long events (MLEs; 5–9 days) and extremely long events (ELEs; ≥ 10 days) to assess how and why certain events persist for far longer than the typical duration. Notably, ELEs exhibited an extended maintenance phase during which high temperatures remained sustained rather than declined. To systematically analyze the differences, we adopted a stage-based comparative framework and evaluated the roles of key local thermodynamic processes—advection, adiabatic and diabatic heating and the surface energy budget—in sustaining and terminating extremely high temperatures. Our findings offer new insights into the thermodynamic characteristics that distinguish ELEs from MLEs under persistent high-pressure systems, thereby enhancing our understanding of the drivers behind exceptionally prolonged heat waves.

This paper is organised as follows. Section 2 describes the observational and reanalysis data, the analysis method and the definition of a heat wave. Section 3 outlines the categorization of heat waves into MLEs and ELEs based on duration and presents the stage-based characteristics of temporal evolution, atmospheric circulation patterns and thermodynamic processes. Section 4 concludes this study with a discussion.

2 | Data and Methods

2.1 | Observational and Reanalysis Data

To define heat waves over South Korea, we used the daily maximum temperature (T_{max}) from the Automated Synoptic Observing System (ASOS) operated by the Korea Meteorological Administration (KMA). The data were collected from 61 stations for 52 summer seasons (June–August) from 1973 to 2024.

The area-averaged T_{max} from these stations was used as a representative value for South Korea.

Meteorological conditions were derived from the 6-hourly Japanese Reanalysis for Three Quarters of a Century (JRA-3Q; Kosaka et al. 2024) dataset, which consists of 37 pressure levels with a horizontal resolution of 1.25°×1.25°. The 6-hourly JRA-3Q data for the following variables were aggregated into daily values: 2-m air temperature (T2m), air temperature (T) at 975 hPa, geopotential height (GPH) at 500 and 200 hPa, vertical velocity (ω) at 500 hPa, specific humidity (Q) at 975 hPa and zonal (U) and meridional winds (V) at 975 hPa. Additional JRA-3Q variables used in this study were the surface energy budget components, total cloud cover, soil moisture and daily precipitation.

To investigate the role of diabatic heating, we further used diabatic heating components at 975 hPa, following Lopez et al. (2025). The following heating rates are explicitly provided in JRA-3Q, but they are not fully available in ERA5: sensible heat transfer without phase change, represented by the vertical diffusion heating rate (VDFHR); latent heat associated with moisture processes, represented by the convective heating rate (CNVHR) and large-scale condensation heating rate (LRGHR); and net atmospheric radiation, represented by the longwave radiative heating rate (LWHR) and solar radiative heating rate (SWHR).

2.2 | Methods

To explore the local temperature evolution associated with heat waves, the thermodynamic energy equation in the pressure coordinates (Holton and Hakim 2013) was used:

$$\frac{\partial T}{\partial t} = -V \cdot \nabla T + S_p \omega + \frac{\dot{Q}}{C_p} \quad (1)$$

where T is the temperature, V is the horizontal wind vector, S_p is the static stability parameter, ω is the vertical velocity in pressure coordinates, $\dot{Q}$ is the diabatic heating and C_p is the specific heat capacity of air at a constant pressure. The terms of Equation (1) from left to right represent the temperature tendency and changes in temperature due to horizontal advection, adiabatic heating and diabatic heating, respectively. The temperature tendency, horizontal advection and adiabatic heating were calculated from the data using their analytical expressions. Note that diabatic heating was estimated as a residual of Equation (1). Equation (1) was evaluated at 975 hPa due to its proximity to the surface, which means that it appropriately represents near-surface thermodynamic processes (González-Herrero et al. 2022; Ha et al. 2022).

To clarify the roles of teleconnection patterns in sustaining prolonged heat waves, we analysed several key teleconnection indices at a daily time scale. The AO index was obtained from the National Oceanic and Atmospheric Administration Climate Prediction Center (NOAA CPC), available at: https://www.cpc.ncep.noaa.gov/products/precip/CWlink/daily_ao_index/ao.shtml. The CGT index was calculated as the regional mean of 200 hPa GPH anomalies over northwestern India (35°–40° N, 60°–70° E) (Ding and Wang 2005). The PJ index was computed as the difference in normalised 850 hPa GPH anomalies between grid points over Taiwan (22° N, 120° E) and Japan (35° N, 140° E) (Kubota et al. 2016).

We conducted a composite analysis to identify the characteristics of two types of heat wave events. Composite anomalies were calculated by subtracting the daily climatological mean of each variable from 1973 to 2024 to exclude seasonal cycles. The statistical significance of the composites was evaluated using a one-sided Student's t-test.

2.3 | Definition of a Heat Wave

A heat wave is generally described as a period of consecutive days in which the air temperature is higher than usual (Smith et al. 2013; Coughlan De Perez et al. 2023). However, more specific definitions of heat waves require that thresholds vary by country due to their differing local climates. In South Korea, the KMA uses an absolute threshold to formally define a heat wave as a period of at least two consecutive days during which T_{max} exceeds 33°C. However, using an absolute threshold is unlikely to detect heat wave events in early or late summer because they are primarily concentrated within a specific period (mid-July to August). To account for the local climate, we here defined a heat wave using a relative threshold (i.e., T_{max} exceeding the seasonally varying 90th percentile threshold for at least two consecutive days). The 90th percentile threshold was calculated for each calendar day during the summer season using T_{max} within a 15-day window centered on the target date based on the reference period of 1981–2010 (Stefanon et al. 2012; Russo et al. 2014).

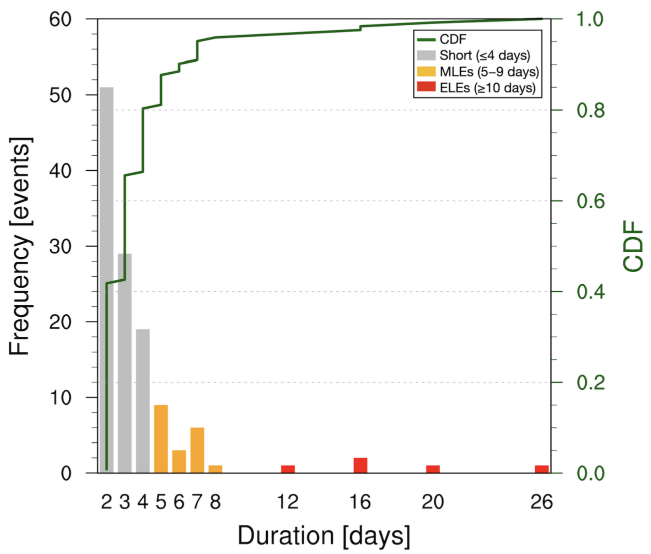

FIGURE 1 | Histogram and cumulative distribution function (CDF; green line) of heat wave events over South Korea during summer months (June 1 to August 31) from 1973 to 2024, categorised by event duration. Coloured bars indicate short-duration events (grey), moderately long events (MLEs; orange) and extremely long events (ELEs; red).

3 | Results

3.1 | Categorization of Duration-Dependent Heat Waves

According to the method for defining heat waves described in Section 2.3, 123 heat wave events were detected over South Korea from 1973 to 2024. Figure 1 shows the distribution of summer heat wave durations, which from 2 to 26 days during that 52-year period. Notably, no events were observed with durations between 9 and 11 days. To establish a statistically robust classification, we analyzed the cumulative distribution function of heat wave durations (right axis in Figure 1). Given that the 80th percentile corresponded to a duration of 4 days, we distinguished long-duration events (lasting 5 days or more) from short-duration events (less than 5 days), following previous studies (Yang et al. 2021; Ji and Chen 2024). Short-duration events were excluded from the analysis because they are typically associated with small-scale or transient high-pressure systems that are largely irrelevant to the sustained thermodynamic processes that are our focus in this study.

Among the remaining long-duration events (≥ 5 days), we classified the most persistent and exceptional heat wave events using a 10-day threshold. This threshold was supported not only by the observed gap in event durations but also by previous research showing that heat waves lasting 10 days or more are often associated with highly stable and persistent atmospheric circulation patterns, such as prolonged blocking or quasi-resonant amplification (Petoukhov et al. 2013; Mann et al. 2018).

Accordingly, we defined MLEs as those lasting between 5 and 9 days (15.4% of the total events) and ELEs as those lasting 10 days or more (top 4.1%). Based on that classification, 24 long heat wave events were identified: 19 MLEs accounting for 113 heat wave days and 5 ELEs accounting for 90 days (Table 1). Despite their low frequency, MLEs and ELEs collectively accounted for 40% of the total heat wave days and exhibited significantly greater intensity than short-duration events. It should be noted that this classification was introduced to facilitate a comparative analysis of representative cases with distinct durations rather than to establish fixed types of heat waves. Our choice of duration thresholds does not affect the robustness of the primary conclusions drawn in this study. For example, in 2024, an ELE was formally followed by an MLE owing to a single day that did not meet the threshold; however, regarding them

TABLE 1 | Summary statistics of summer heat wave events over South Korea from 1973 to 2024, categorised by duration: Short-duration events (2–4 days), moderately long events (MLEs; 5–9 days), and extremely long events (ELEs; ≥ 10 days). The average intensity is defined as the mean daily T_{max} anomaly relative to the 90th percentile threshold.

Category	Frequency [events]	Proportion [%]	Total days [days]	Average duration [days]	Average intensity [°C]
Short (2–4 days)	99	80.5	265	2.7	0.80
MLEs (5–9 days)	19	15.4	113	5.9	0.95
ELEs (≥ 10 days)	5	4.1	90	18.0	1.44
Total	123	100	468	3.8	0.96

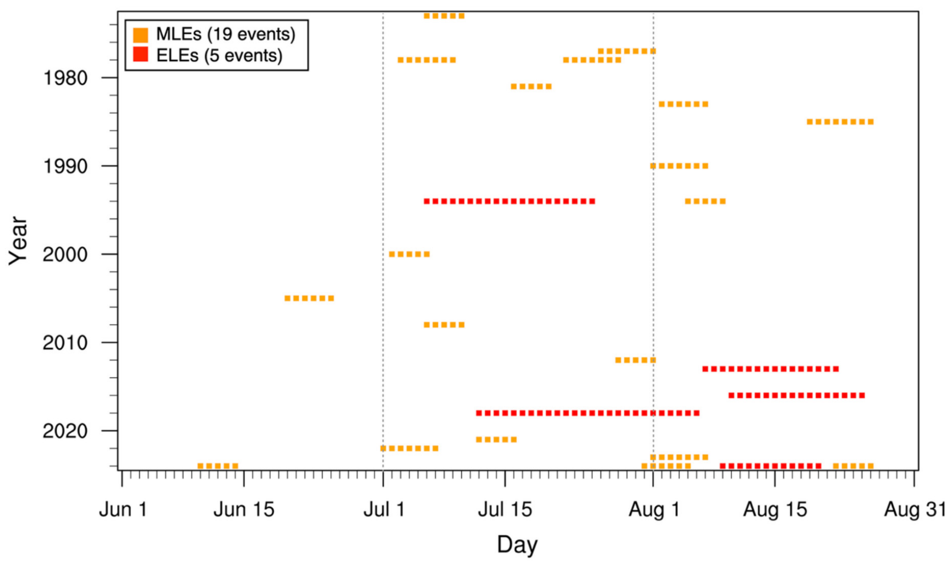

FIGURE 2 | Temporal distribution of heat wave events based on daily maximum temperature (T_{max}) for moderately long events (MLEs; 5–9 days) and extremely long events (ELEs; ≥ 10 days). Coloured squares represent MLEs (orange) and ELEs (red).

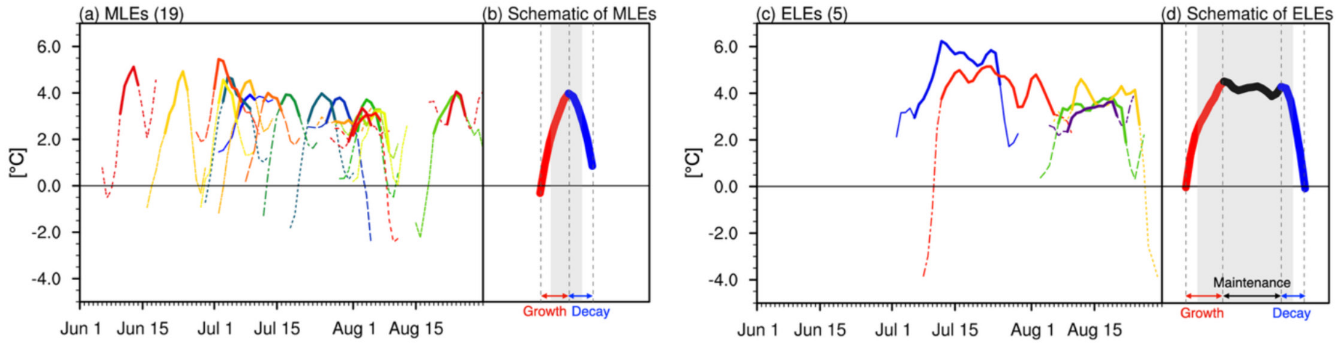

FIGURE 3 | (a, c) Temporal evolution of daily maximum temperature (T_{max}) anomalies (°C, relative to the daily climatology of 1973–2024), area-averaged over South Korea (34°–38° N, 125°–130° E) for moderately long events (MLEs; 5–9 days) and extremely long events (ELEs; ≥ 10 days). Coloured dotted lines represent T_{max} from day −5 to day +5 relative to the onset and end dates of individual heat wave events. Thick lines indicate the duration of heat wave events. (b, d) Schematic diagrams showing composite-mean T_{max} anomalies evolution for MLEs and ELEs. Thick red, black, and blue lines represent the growth, maintenance and decay stages, respectively. Grey shading denotes the duration of the heat wave event. Numbers in parentheses indicate the number of events.

as a single continuous ELE yields consistent results, demonstrating the robustness of our classification.

Figure 2 illustrates the temporal distribution of heat waves over South Korea during the 52 summer seasons from 1973 to 2024. MLEs and ELEs predominantly occurred in July and August, whereas short-duration events were more evenly distributed throughout the summer. ELEs were primarily concentrated in late summer from mid-July to August. On average, ELEs exhibited a difference of 1.44°C between their daily T_{max} and the seasonally varying 90th percentile threshold, which is notably greater than the 0.95°C observed for MLEs (Table 1). This indicates that despite fewer occurrences (only 5 cases), ELEs have a substantial effect due to both their duration and intensity.

The longest heat wave, lasting for 26 days, occurred in July–August 2018. Other ELEs were observed in 1994 (20 days), 2013 (16 days), 2016 (16 days) and 2024 (12 days). These events are consistent with the record-breaking heat waves reported in previous studies (Yeh et al. 2018; Min, Kim, et al. 2020; Ha et al. 2020). Notably, four out of the five ELEs occurred since the 1990s, indicating a recent trend toward longer-lasting heat waves. Despite their rarity, this trend suggests a potential increase due to ongoing global warming and underscores the need to better understand the physical processes that sustain their persistence.

3.2 | Stage-Based Characteristics of MLEs and ELEs

3.2.1 | Temporal Evolution

We examined the temporal evolution of heat waves with different durations by comparing MLEs and ELEs. Figure 3a,c shows area-averaged T_{max} anomalies (relative to the daily climatology of 1973–2024) over South Korea (34°–38° N, 125°–130° E) within a 5-day window before and after the onset and end of individual MLE and ELE events (coloured dotted lines). MLEs exhibited a largely symmetrical temperature evolution around the event onset. T_{max} anomalies began increasing significantly before the event onsets, peaking shortly after onset and then decreased rapidly as the event ended, returning to the climatological levels. Conversely, although ELEs showed similar initial growth, they featured a distinct maintenance phase during which T_{max} anomalies remained up to 4.2°C above normal with slight fluctuations before gradually returning to normal.

To perform detailed research on the full life cycles of these events, we classified each heat wave event into stages based on its temperature evolution: the growth stage, defined as the period of rapid temperature increase before onset (5.8 days on average for MLEs, 8 days for ELEs); the maintenance stage, during which temperature remained relatively stable at a high level (10.2 days for ELEs, not present in MLEs); and the decay stage, marked by a rapid temperature decrease after the peak of the event (3.8 for MLEs, 3.6 days for ELEs) (Figure 3b,d). Notably, MLEs comprised only the growth and decay stages, whereas ELEs included all three, highlighting the presence of a sustained high-temperature phase unique to ELEs. This stage-based framework was introduced to better capture the dynamic evolution of heat waves. Note that the analysis period is different for each heat wave event to reflect the event-specific temporal evolution of T_{max} anomalies. The following analyses focus on the characteristics of each stage for MLEs and ELEs.

3.2.2 | Atmospheric Patterns

Although this study focuses on thermodynamic characteristics, it is essential to examine the background circulation patterns that initiate and maintain heat waves. To clarify that, we conducted a stage-based composite analysis of anomalous GPH at 500, ω at 500, Q at 975 and UV at 975 hPa (Figure 4). In addition, we examined the normalised indices of three key teleconnection patterns (PJ, CGT and AO) during each stage because they are widely recognised as remote drivers of heat waves (Lee and Lee 2016; Kim et al. 2022; Kim et al. 2024; Table 2).

Given that MLEs and ELEs both lasted more than 5 days, the MLEs shared several initial features with the ELEs during the

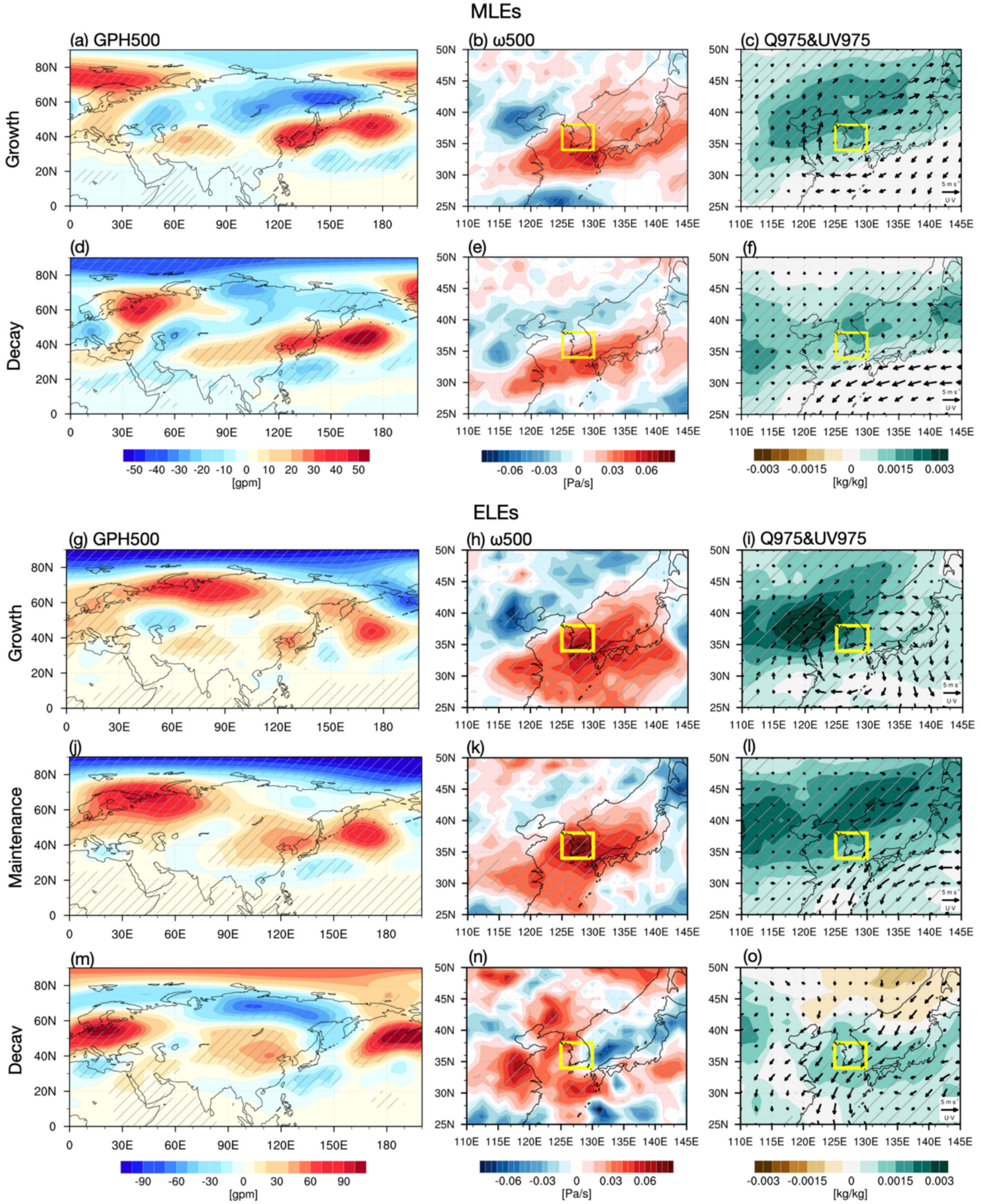

FIGURE 4 | Composite anomalies of (left) geopotential height (GPH, gpm) at 500 hPa, (center) vertical velocity (ω, Pa/s) at 500 hPa and (right) specific humidity (Q, kg/kg) and wind vectors (UV, m/s) at 975 hPa for (a–f) moderately long events (MLEs; 5–9 days) and (g–o) extremely long events (ELEs; ≥ 10 days). The yellow box denotes the region of South Korea (34°–38° N, 125°–130° E). Statistically significant anomalies at a 95% confidence level are indicated by hatched areas.

TABLE 2 | Normalised PJ, CGT and AO indices during different heat wave stages for moderately long events (MLEs; 5–9 days) and extremely long events (ELEs; ≥ 10 days).

Index	MLEs		ELEs		
	Growth	Decay	Growth	Maintenance	Decay
PJ	0.24*	0.37**	0.05	−0.04	0.02
CGT	0.59*	0.11	0.68*	0.00	0.18
AO	−0.04	0.17*	0.44**	0.74**	0.71**

Note: *$p < 0.5$, **$p < 0.01$.

growth stage, including high-pressure systems over East Asia, local subsidence and southwesterly winds (Figure 4a–c). A broader wave train structure that extended from Europe to the southern region of the Kamchatka Peninsula was indicative of an eastward-propagating Rossby wave (Ding and Wang 2005; Yeo et al. 2019), which was associated with a significantly positive CGT index (+0.59, $p < 0.05$; Table 2). Furthermore, a north–south dipole pattern, consisting of an East Asian high and a Russian low, corresponded to a weak but positive PJ index (+0.24, $p < 0.05$), reflecting localized wave activity over the western North Pacific and Japan (Nitta 1987; Noh et al. 2021). The resulting high-pressure system over South Korea induced broad subsidence. In the lower troposphere, southwesterly winds transported warm and moist air from the East China Sea and western Pacific to South Korea, creating thermodynamic conditions favorable for the development of heat waves. As each event decayed (Figure 4d–f), the high-pressure system weakened, leading to reduced subsidence and weaker low-level southerly winds. These changes primarily contributed to the dissipation of MLEs.

Compared with MLEs, ELEs featured more robust and persistent high-pressure systems throughout their life cycles. During their growth (Figure 4g–i), a slightly more amplified high-pressure system developed over South Korea, with concurrent low-pressure systems in the Arctic (above 80° N), corresponding to a significantly positive AO phase (+0.44, $p < 0.01$). Such low anomalies over the Arctic intensified the Arctic–midlatitude temperature gradient, which in turn induced a northward shift of the jet stream. Consequently, the westerlies weakened over East Asia, favouring the persistence of the high-pressure system over South Korea (Lee and Lee 2016; Wu and Francis 2019; Lee, Noh, et al. 2024). Additionally, at 200 hPa, a more distinct CGT-like pattern, with high and low features over the mid-latitudes, was observed when the CGT index was significantly positive (+0.68, $p < 0.05$) (not shown). This suggests that large-scale wave activity contributed to the amplification of high-pressure systems over East Asia, which in turn supported local subsidence.

During the maintenance stage (Figure 4j–l), high-pressure systems intensified and persisted from Western Europe to East Asia. Even though the CGT index dropped to near zero, the continued positive phase of the AO (+0.74, $p < 0.01$) helped sustain high-pressure systems established during the growth stage. Additionally, an anomalous high-pressure system over the southern Kamchatka Peninsula acted as an atmospheric blocking, hindering the eastward progression of the high-pressure system over Korea (Yeh et al. 2018; Min, Chung, et al. 2020). Although individual ELEs originated from diverse forcings—such as blocking highs over the Kamchatka Peninsula in 2016 (Yoon et al. 2021) or the westward expansion of the Western North Pacific Subtropical High in 1994 and 2018 (Ha et al. 2020)—they consistently resulted in a prolonged high-pressure system over South Korea, supporting strong subsidence and weak low-level winds. In the decay stage (Figure 4m–o), the high-pressure systems gradually weakened and shifted westward despite a strongly positive AO index (+0.71, $p < 0.01$). This is because the AO reflects the Arctic–midlatitude dipole structure, which does not always align with regional anomalies. The weakening of the high-pressure system over Korea facilitated northeasterly winds into the Korean Peninsula, which advected dry and cold air and thereby contributed to the decay of ELEs.

Taken together, these results show that ELEs are associated with distinct atmospheric circulation patterns that are strongly linked to persistent Arctic forcing. However, circulation differences alone do not fully explain their contrasting thermodynamic characteristics. The following sections examine how local thermodynamic processes further distinguish the duration of heat waves, highlighting that ELEs are not merely prolonged MLEs but involve fundamentally different mechanisms.

3.2.3 | Thermodynamic Characteristics

Having established the presence of high-pressure systems during MLEs and ELEs, we used the thermodynamic energy equation in pressure coordinates (Equation 1) to quantify the contributions of thermodynamic processes to temperature changes at 975 hPa, spatially averaged over South Korea (34°–38° N, 125°–130° E) across each stage of these events (Figure 5). We found that ELEs differed from MLEs in two key thermodynamic characteristics. First, although both MLEs and ELEs exhibited similar initial temperature increases driven by warm horizontal advection and adiabatic heating associated with strong subsidence, ELEs sustained that warming for longer due to prolonged subsidence under persistent high-pressure systems. Second, during the decay stage, although high-pressure systems weakened in both cases, ELEs exhibited an insignificant but positive diabatic contribution that was absent in MLEs.

During the growth stage of MLEs, positive temperature tendency was primarily driven by horizontal advection associated with anomalous southwesterly winds transporting moisture from the ocean (Figure 5a). Those southwesterly winds were influenced

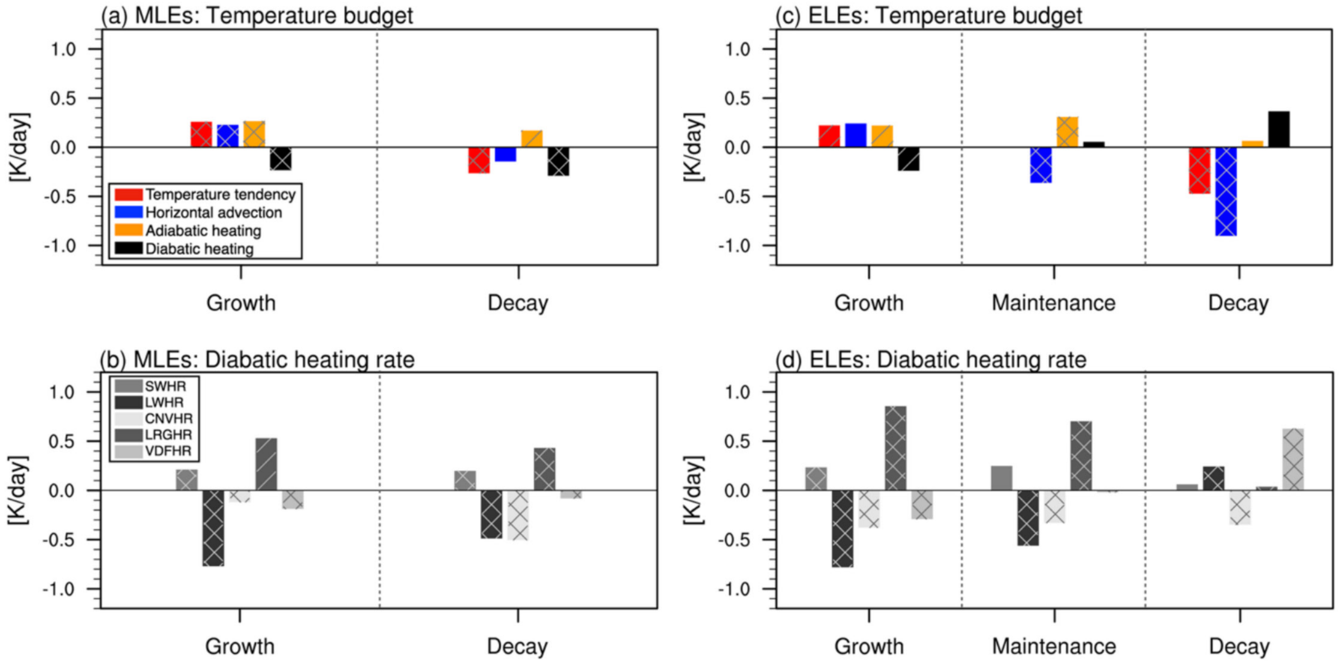

FIGURE 5 | Bar graphs of anomalous (a, c) temperature budget components and (b, d) diabatic heating rate at 975 hPa, area-averaged over South Korea (34°–38° N, 125°–130° E), during different heat wave stages in (a, b) moderately long events (MLEs; 5–9 days) and (c, d) extremely long events (ELEs; ≥ 10 days). The top panels show temperature budget components: Total temperature tendency (red), horizontal advection (blue), adiabatic heating (orange) and diabatic heating (black). The bottom panels show components of the diabatic heating rate from JRA-3Q: Shortwave radiative heating rate (SWHR), longwave radiative heating rate (LWHR), convective heating rate (CNVHR), large-scale condensation heating rate (LRGHR) and vertical diffusion heating rate (VDFHR). Statistically significant anomalies at the 95% (99%) confidence level are indicated by grey hatched (cross-hatched) areas.

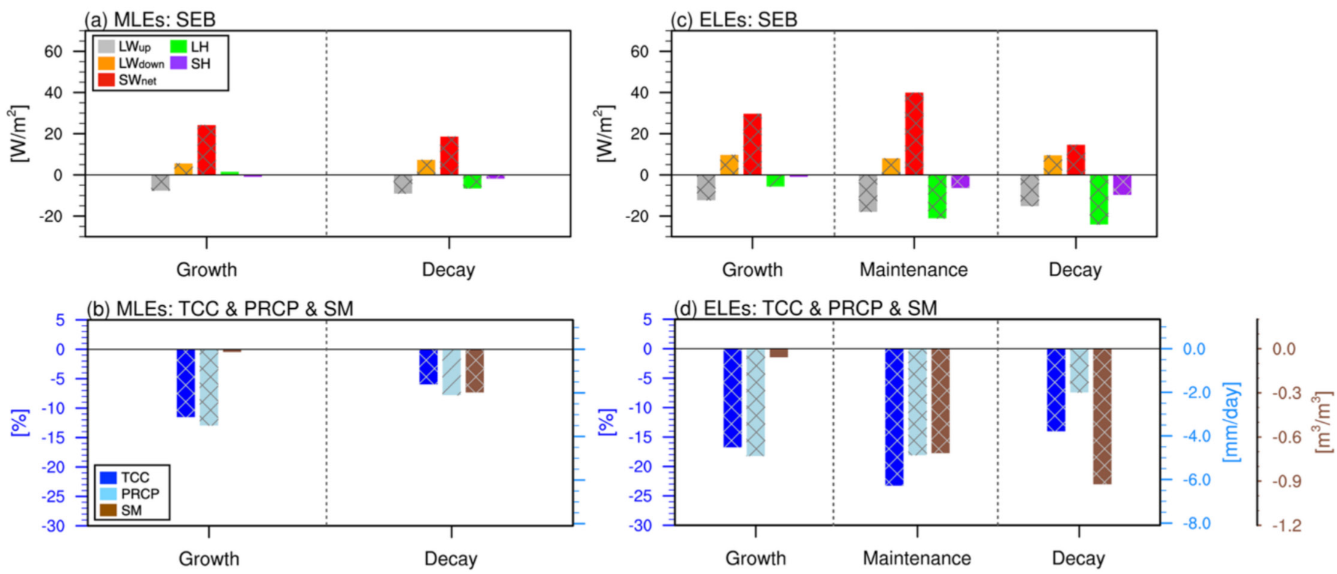

FIGURE 6 | Bar graphs of anomalous (a, c) surface energy budget (SEB) components and (b, d) total cloud cover (TCC), daily precipitation (PRCP) and soil moisture (SM), area-averaged over South Korea (34°–38° N, 125°–130° E), during different heat wave stages for (a, b) moderately long events (MLEs; 5–9 days) and (c, d) extremely long events (ELEs; ≥ 10 days). The SEB components are upward longwave radiation flux (LW_{up}; grey), downward longwave radiation flux (LW_{down}; orange), net shortwave radiation flux (SW_{net}; red), latent heat flux (LH; green) and surface sensible heat flux (SH; purple). In panels (b, d), TCC (blue; left axis), PRCP (sky blue; right axis) and SM (brown; right axis) anomalies are shown. A positive value indicates downward. Statistically significant anomalies at the 95% (99%) confidence level are indicated by grey hatched (cross-hatched) areas.

by a developing high-pressure system centered over the East Sea (Figure 4a,c). As the high-pressure system intensified, adiabatic heating from increased subsidence and enhanced surface net shortwave radiation due to reduced cloud cover significantly amplified the warming (Figures 5a and 6a). Enhanced downward longwave radiation due to abundant moisture further supported this process. The net diabatic heating, on the other hand, acted as a damping term, partially offsetting the warming. This damping was primarily due to LWHR, which was associated with emitted longwave radiation from the warmed atmosphere (Figure 5b). CNVHR and VDFHR further contributed to diabatic cooling by limiting convective heat and vertical heat transport under the influence of strong subsidence.

As MLEs transitioned into the decay stage, the temperature tendency reversed, primarily due to diabatic cooling from CNVHR and LWHR. The weakening of the high-pressure system and associated subsidence disrupted the anomalous southwesterly winds and induced cold horizontal advection, but its influence was not statistically significant ($p > 0.05$; Figures 4f and 5a).

In ELEs, the growth stage resembled that of MLEs, but the maintenance and decay stages exhibited distinct thermodynamic characteristics (Figure 5c). During the maintenance stage, which was prominent during ELEs, the temperature tendency was near zero, indicating the persistence of extremely high temperature anomalies. This balance arose from adiabatic heating associated with strong subsidence and compensating cold horizontal advection induced by anomalous northeasterlies (Figure 4j–l). Meanwhile, diabatic heating began to contribute positively, likely reflecting surface-induced warming. Persistent subsidence suppressed cloud formation, increasing surface shortwave radiation income (Figure 6c). As a result, the release of both sensible and latent heat fluxes increased, suggesting stronger land–atmosphere interaction. This was accompanied by a marked decline in soil moisture, likely reflecting cumulative surface drying due to sustained evaporation (Figure 6d).

During the decay stage, strong cold horizontal advection and weakened adiabatic heating dominated the negative temperature tendency. This shift was due to the westward movement of high-pressure systems, which brought cold and dry air through northeasterly winds (Figure 4m–o). In contrast, the positive contribution of diabatic heating increased, delaying the decay of ELEs, although not by a statistically significant amount ($p > 0.05$). This increase was partly due to enhanced VDFHR, which reflected upward heat transport due to released sensible heat flux (Figure 5d). The surface energy budgets support this result, showing reduced net shortwave radiation but increased sensible heat flux (Figure 6c). Notably, soil moisture did not recover to climatological levels after the events, implying prolonged surface dryness. This could not only intensify heat waves but also create favourable conditions for concurrent or subsequent droughts (Li et al. 2019; Seo and Ha 2022).

These results suggest that ELEs are not merely responses to persistent high-pressure systems. Although large-scale circulation (e.g., CGT and AO) initiated ELEs by providing the necessary atmospheric background, including persistent upper-level high-pressure systems, the maintenance of extremely high temperatures in ELEs was further supported by thermodynamic processes involving land–atmosphere interactions. Sustained sensible heat release under continued drying distinguished ELEs from MLEs, in which subsidence weakened and the surface recovered more quickly, limiting their duration.

4 | Discussion and Conclusion

In this study, we compared the thermodynamic characteristics of recent ELEs (≥ 10 days) with those of MLEs (5–9 days) in South Korea. By adopting a stage-based analysis framework, we systematically examined the life cycles of heat wave events, their growth, maintenance and decay stages, to better understand the physical processes that modulate heat wave persistence.

The thermodynamic evolution of MLEs and ELEs revealed both commonalities and key distinctions. The growth stage of both event types exhibited initial warming dominated by horizontal warm advection, with adiabatic heating as high-pressure systems intensified. However, their development diverged in the later stages. MLEs decayed as the high-pressure system weakened, allowing enhanced cold advection and diabatic cooling. In contrast, ELEs featured a prolonged maintenance stage in which persistent high-pressure systems sustained adiabatic warming and promoted increasing diabatic heating, particularly through intensified land–atmosphere interactions. In particular, gradual soil moisture depletion enhanced sensible heat flux, which, together with vertical diffusion heating, contributed to maintaining elevated temperatures. Even as circulation began to shift and cold advection intensified, enhanced diabatic heating continued to counteract cooling, delaying the termination of ELEs.

A key finding of this study is that ELEs are not merely extended versions of MLEs but possess qualitatively distinct thermodynamic characteristics, particularly during the maintenance stage. Although large-scale circulation (e.g., CGT and AO) initiates ELEs by providing favourable conditions for persistent high-pressure systems, regional thermodynamic processes increasingly dominate their persistence. In particular, surface drying suppresses the rapid decay of ELEs by enhancing the release of sensible heat flux to the atmosphere, which can reinforce high-pressure anomalies and form a sustaining cycle of dryness and warming (Seo et al. 2021; Yoon et al. 2023; Lyu et al. 2024).

Although those processes have been well documented in continental areas such as Eurasia, their increasing relevance over the Korean Peninsula, traditionally considered a region with limited land–atmosphere interactions due to its relatively humid and oceanic climate, suggests a possible shift in heat wave characteristics. This shift might reflect observed trends such as soil moisture depletion, which could further enhance land–atmosphere feedback under future climate conditions (Cheng et al. 2015; Li et al. 2021). Nonetheless, given the complexity of these interactions, further long-term and high-resolution observations are needed to enhance our understanding and improve the prediction of future heat wave events.

Although our results highlight the role of thermodynamic processes in prolonging heat waves, our circulation-based composite analysis further indicates that large-scale teleconnection patterns, such as the CGT and AO, modulate the synoptic circulations that support the development and maintenance of heat waves. Although we did not quantitatively assess the relative contributions of each teleconnection pattern, the consistent association between a positive AO phase and ELEs indicates a possible link between remote forcings and heat wave persistence (Lee and Lee 2016; Wu and Francis 2019). In addition, Choi et al. (2020) reported significant decadal shifts in the interannual variability of heat waves in East Asia that were linked to an amplified Scandinavian teleconnection pattern. Those findings, together with growing evidence that local topographic forcing and slowed Rossby wave propagation contribute to prolonging heat waves (Jiménez-Esteve et al. 2022; Nie et al. 2024), highlight the need for further studies to systematically assess how remote forcings and their variability modulate the persistence of ELEs under both present and future climate conditions.

In conclusion, our findings indicate that the recently prolonged heat waves in South Korea should be distinguished from others in terms of their thermodynamic processes. Specifically, the combined influence of adiabatic heating associated with persistent upper-level high-pressure anomalies and diabatic heating involving land–atmosphere interactions plays a critical role in prolonging heat waves. Although the number of observed ELEs remains small, their frequency is projected to increase with ongoing climate change. In this regard, our study provides insights into the processes governing the persistence of such extreme heat events. Expanding the sample size and conducting comparative analyses across similar climate zones would enhance the robustness and generalizability of these findings. Furthermore, incorporating model simulations or scenario-based analyses could enhance understanding of external influences, such as anthropogenic forcing, on heat waves during global warming. Such integrative approaches will ultimately support more accurate predictions and improved preparedness for future extreme heat waves in South Korea and beyond.

Author Contributions

Minjeong Cho: writing – original draft, investigation, data curation, formal analysis, validation, visualization. **Ha-Rim Kim:** writing – review and editing, investigation, methodology, conceptualization. **Changhyun Yoo:** methodology, conceptualization, writing – review and editing. **Yong-Sang Choi:** writing – review and editing, supervision, funding acquisition.

Acknowledgements

This research was supported by the Specialized University Program of the Korea Meteorological Institute (KMI). This research was also supported by the Basic Science Research Program through the National Research Foundation of Korea (NRF), funded by the Ministry of Education (2018R1A6A1A08025520) and by a National Research Foundation of Korea (NRF) grant funded by the Korean government (MSIT) (2021R1A2C1093402). Minjeong Cho was supported by an Ewha Womans University scholarship in 2022.

Conflicts of Interest

The authors declare no conflicts of interest.

Data Availability Statement

The data that support the findings of this study are available from the corresponding author upon reasonable request.

References

Allan, R. P., P. A. Arias, S. Berger, et al. 2023. "Intergovernmental Panel on Climate Change (IPCC)." In *Summary for Policymakers. Climate Change 2021: The Physical Science Basis. Contribution of Working Group I to the Sixth Assessment Report of the Intergovernmental Panel on Climate Change*. Cambridge University Press.

Bador, M., L. Terray, J. Boé, et al. 2017. "Future Summer Mega-Heatwave and Record-Breaking Temperatures in a Warmer France Climate." *Environmental Research Letters* 12: 74025.

Barriopedro, D., R. García-Herrera, C. Ordóñez García, D. G. Miralles, and S. Salcedo-Sanz. 2023. "Heat Waves: Physical Understanding and Scientific Challenges." *Reviews of Geophysics* 61: e2022RG000780.

Chen, R., J. Liu, S. Tang, and X. Li. 2024. "Spatially Compounding Flood-Nocturnal Heat Events Over Adjacent Regions in the Northern Hemisphere." *Npj Climate and Atmospheric Science* 7: 237.

Chen, R., Z. Wen, R. Lu, and W. Liu. 2021. "Interdecadal Changes in the Interannual Variability of the Summer Temperature Over Northeast Asia." *Journal of Climate* 34: 8361–8376.

Cheng, S., X. Guan, J. Huang, F. Ji, and R. Guo. 2015. "Long-Term Trend and Variability of Soil Moisture Over East Asia." *Journal of Geophysical Research: Atmospheres* 120: 8658–8670.

Choi, N., M.-I. Lee, D.-H. Cha, Y.-K. Lim, and K.-M. Kim. 2020. "Decadal Changes in the Interannual Variability of Heat Waves in East Asia Caused by Atmospheric Teleconnection Changes." *Journal of Climate* 33: 1505–1522.

Choi, W., C.-H. Ho, J. Jung, M. Chang, and K.-J. Ha. 2021. "Synoptic Conditions Controlling the Seasonal Onset and Days of Heatwaves Over Korea." *Climate Dynamics* 57: 3045–3053.

Coughlan De Perez, E., J. Arrighi, and J. Marunye. 2023. "Challenging the Universality of Heatwave Definitions: Gridded Temperature Discrepancies Across Climate Regions." *Climatic Change* 176: 167.

De Polt, K., P. J. Ward, M. De Ruiter, et al. 2023. "Quantifying Impact-Relevant Heatwave Durations." *Environmental Research Letters* 18: 104005.

Ding, Q., and B. Wang. 2005. "Circumglobal Teleconnection in the Northern Hemisphere Summer." *Journal of Climate* 18: 3483–3505.

Domeisen, D. I., E. A. Eltahir, E. M. Fischer, et al. 2023. "Prediction and Projection of Heatwaves." *Nature Reviews Earth and Environment* 4: 36–50.

García-Herrera, R., J. Díaz, R. M. Trigo, J. Luterbacher, and E. M. Fischer. 2010. "A Review of the European Summer Heat Wave of 2003." *Critical Reviews in Environmental Science and Technology* 40: 267–306.

González-Herrero, S., D. Barriopedro, R. M. Trigo, J. A. López-Bustins, and M. Oliva. 2022. "Climate Warming Amplified the 2020 Record-Breaking Heatwave in the Antarctic Peninsula." *Communications Earth & Environment* 3: 122.

Ha, K.-J., Y.-W. Seo, J.-H. Yeo, et al. 2022. "Dynamics and Characteristics of Dry and Moist Heatwaves Over East Asia." *Npj Climate and Atmospheric Science* 5: 49.

Ha, K.-J., J.-H. Yeo, Y.-W. Seo, et al. 2020. "What Caused the Extraordinarily Hot 2018 Summer in Korea?" *Journal of the Meteorological Society of Japan Ser II* 98: 153–167.

Ho, H. C., K. M. Wai, M. He, T.-C. Chan, C. Deng, and M. S. Wong. 2020. "Mortality Risk of a Future Heat Event Across a Subtropical City: Implications for Community Planning and Health Policy." *Natural Hazards* 103: 623–637.

Holton, J. R., and G. J. Hakim. 2013. *An Introduction to Dynamic Meteorology*. Academic press.

Iwasaki, Y., K. Kasai, K. Hirukawa, and M. Kawakami. 2019. "The Impact of Japan Heatwave on Community Emergency Medicine in 2018." *Prehospital and Disaster Medicine* 34: s29–s30.

Ji, L., and H. Chen. 2024. "Differences in Variations of Long-Lived and Short-Lived Summer Heat Waves During 1981–2020 Over Eastern

China and Their Corresponding Large-Scale Circulation Anomalies." *Journal of Meteorological Research* 38: 414–436.

Jiménez-Esteve, B., K. Kornhuber, and D. Domeisen. 2022. "Heat Extremes Driven by Amplification of Phase-Locked Circumglobal Waves Forced by Topography in an Idealized Atmospheric Model." *Geophysical Research Letters* 49: e2021GL096337.

Kim, D. S., S. Y. Jun, M. I. Lee, and J. S. Kug. 2022. "Significant Relationship Between Arctic Warming and East Asia Hot Summers." *International Journal of Climatology* 42: 9530–9538.

Kim, H., N. Choi, M.-I. Lee, S. Tak, D.-H. Cha, and S.-K. Min. 2024. "Causes on the 2018 Record-Breaking Heatwave in South Korea: Compound Impacts From Recurrent Large-Scale Atmospheric Teleconnections." *Environmental Research Letters* 19: 124064.

Kim, J., D.-G. Lee, and J. Kysely. 2008. "A Synoptic and Climatological Comparison of Record-Breaking Heat Waves in Korea and Europe." *Atmosphere* 18: 355–365.

Kim, M. K., J. S. Oh, C. K. Park, S. K. Min, K. O. Boo, and J. H. Kim. 2019. "Possible Impact of the Diabatic Heating Over the Indian Subcontinent on Heat Waves in South Korea." *International Journal of Climatology* 39: 1166–1180.

Kim, Y.-H., S.-K. Min, D. A. Stone, H. Shiogama, and P. Wolski. 2018. "Multi-Model Event Attribution of the Summer 2013 Heat Wave in Korea." *Weather and Climate Extremes* 20: 33–44.

Kosaka, Y., S. Kobayashi, Y. Harada, et al. 2024. "The JRA-3Q Reanalysis." *Journal of the Meteorological Society of Japan Ser II* 102: 49–109.

Kubota, H., Y. Kosaka, and S. P. Xie. 2016. "A 117-Year Long Index of the Pacific-Japan Pattern With Application to Interdecadal Variability." *International Journal of Climatology* 36: 1575–1589.

Kysely, J., and J. Kim. 2009. "Mortality During Heat Waves in South Korea, 1991 to 2005: How Exceptional Was the 1994 Heat Wave?" *Climate Research* 38: 105–116.

Lee, H.-D., K.-H. Min, J.-H. Bae, and D.-H. Cha. 2020. "Characteristics and Comparison of 2016 and 2018 Heat Wave in Korea." *Atmosphere* 30: 1–15.

Lee, M.-H., E. Noh, J.-H. Kim, J. Kim, and S.-Y. Jun. 2024. "Contribution Assessment of Northern Hemispheric Atmospheric Circulations to Korean Mid-Summer Surface Warming by the Atmospheric Nudging Experiment." *Asia-Pacific Journal of Atmospheric Sciences* 60: 119–130.

Lee, W. S., and M. I. Lee. 2016. "Interannual Variability of Heat Waves in South Korea and Their Connection With Large-Scale Atmospheric Circulation Patterns." *International Journal of Climatology* 36: 4815–4830.

Lee, Y., D. Cho, J. Im, et al. 2024. "Unveiling Teleconnection Drivers for Heatwave Prediction in South Korea Using Explainable Artificial Intelligence." *Npj Climate and Atmospheric Science* 7: 176.

Li, K., J. Zhang, K. Yang, and L. Wu. 2019. "The Role of Soil Moisture Feedbacks in Future Summer Temperature Change Over East Asia." *Journal of Geophysical Research: Atmospheres* 124: 12034–12056.

Li, X., G. Ren, Q. You, S. Wang, and W. Zhang. 2021. "Soil Moisture Continues Declining in North China Over the Regional Warming Slowdown of the Past 20 Years." *Journal of Hydrometeorology* 22: 3001–3015.

Lin, W., R. Chen, Z. Wen, and W. Chen. 2022. "Large-Scale Circulation Features Responsible for Different Types of Extreme High Temperatures With Extreme Coverage Over South China." *International Journal of Climatology* 42: 974–992.

Liu, L., Y. Huang, and J. R. Gyakum. 2025. "Clouds Reduce Downwelling Longwave Radiation Over Land in a Warming Climate." *Nature* 637: 868–874.

Lopez, H., S.-K. Lee, R. West, D. Kim, and L. Jia. 2025. "The Longest-Lasting 2023 Western North American Heat Wave Was Fueled by the Record-Warm Atlantic Ocean." *Nature Communications* 16: 6544.

Lyu, Y., J. Wang, X. Zhi, et al. 2024. "The Characterization, Mechanism, Predictability, and Impacts of the Unprecedented 2023 Southeast Asia Heatwave." *Npj Climate and Atmospheric Science* 7: 246.

Ma, F., and X. Yuan. 2021. "More Persistent Summer Compound Hot Extremes Caused by Global Urbanization." *Geophysical Research Letters* 48: e2021GL093721.

Mann, M. E., S. Rahmstorf, K. Kornhuber, et al. 2018. "Projected Changes in Persistent Extreme Summer Weather Events: The Role of Quasi-Resonant Amplification." *Science Advances* 4: eaat3272.

Mazdiyasni, O., M. Sadegh, F. Chiang, and A. Aghakouchak. 2019. "Heat Wave Intensity Duration Frequency Curve: A Multivariate Approach for Hazard and Attribution Analysis." *Scientific Reports* 9: 14117.

Min, K. H., C. H. Chung, J. H. Bae, and D. H. Cha. 2020. "Synoptic Characteristics of Extreme Heatwaves Over the Korean Peninsula Based on ERA Interim Reanalysis Data." *International Journal of Climatology* 40: 3179–3195.

Min, S.-K., Y.-H. Kim, S.-M. Lee, et al. 2020. "Quantifying Human Impact on the 2018 Summer Longest Heat Wave in South Korea." *Bulletin of the American Meteorological Society* 101: S103–S108.

Nie, Y., H.-L. Ren, J. Zuo, et al. 2024. "Eurasian Mid-Latitude Jet Stream Bridges an Atlantic to Asia Summer Teleconnection in Heat Extremes." *Environmental Research Letters* 19: 44003.

Nitta, T. 1987. "Convective Activities in the Tropical Western Pacific and Their Impact on the Northern Hemisphere Summer Circulation." *Journal of the Meteorological Society of Japan Ser II* 65: 373–390.

Noh, E., J. Kim, S. Y. Jun, et al. 2021. "The Role of the Pacific-Japan Pattern in Extreme Heatwaves Over Korea and Japan." *Geophysical Research Letters* 48: e2021GL093990.

Otto, F. E., N. Massey, G. J. Van Oldenborgh, R. G. Jones, and M. R. Allen. 2012. "Reconciling Two Approaches to Attribution of the 2010 Russian Heat Wave." *Geophysical Research Letters* 39: 2011GL050422.

Perkins, S. E. 2015. "A Review on the Scientific Understanding of Heatwaves—Their Measurement, Driving Mechanisms, and Changes at the Global Scale." *Atmospheric Research* 164: 242–267.

Perkins-Kirkpatrick, S., and S. Lewis. 2020. "Increasing Trends in Regional Heatwaves." *Nature Communications* 11: 3357.

Petoukhov, V., S. Rahmstorf, S. Petri, and H. J. Schellnhuber. 2013. "Quasiresonant Amplification of Planetary Waves and Recent Northern Hemisphere Weather Extremes." *Proceedings of the National Academy of Sciences* 110: 5336–5341.

Ren, L., T. Zhou, and W. Zhang. 2020. "Attribution of the Record-Breaking Heat Event Over Northeast Asia in Summer 2018: The Role of Circulation." *Environmental Research Letters* 15: 054018.

Revich, B., and D. Shaposhnikov. 2012. "Climate Change, Heat Waves, and Cold Spells as Risk Factors for Increased Mortality in Some Regions of Russia." *Studies on Russian Economic Development* 23: 195–207.

Robine, J.-M., S. L. K. Cheung, S. Le Roy, et al. 2008. "Death Toll Exceeded 70,000 in Europe During the Summer of 2003." *Comptes Rendus Biologies* 331: 171–178.

Rohini, P., M. Rajeevan, and P. Mukhopadhay. 2019. "Future Projections of Heat Waves Over India From CMIP5 Models." *Climate Dynamics* 53: 975–988.

Russo, S., A. Dosio, R. G. Graversen, et al. 2014. "Magnitude of Extreme Heat Waves in Present Climate and Their Projection in a Warming World." *Journal of Geophysical Research: Atmospheres* 119: 12500–12512.

Seneviratne, S. I., T. Corti, E. L. Davin, et al. 2010. "Investigating Soil Moisture–Climate Interactions in a Changing Climate: A Review." *Earth-Science Reviews* 99: 125–161.

Seo, E., M.-I. Lee, J.-H. Jeong, et al. 2019. "Impact of Soil Moisture Initialization on Boreal Summer Subseasonal Forecasts: Mid-Latitude Surface Air Temperature and Heat Wave Events." *Climate Dynamics* 52: 1695–1709.

Seo, Y.-W., and K.-J. Ha. 2022. "Changes in Land-Atmosphere Coupling Increase Compound Drought and Heatwaves Over Northern East Asia." *Npj Climate and Atmospheric Science* 5: 100.

Seo, Y.-W., K.-J. Ha, and T.-W. Park. 2021. "Feedback Attribution to Dry Heatwaves Over East Asia." *Environmental Research Letters* 16: 064003.

Smith, T. T., B. F. Zaitchik, and J. M. Gohlke. 2013. "Heat Waves in the United States: Definitions, Patterns and Trends." *Climatic Change* 118: 811–825.

Stefanon, M., F. D'andrea, and P. Drobinski. 2012. "Heatwave Classification Over Europe and the Mediterranean Region." *Environmental Research Letters* 7: 14023.

Tak, S., E. Seo, P. A. Dirmeyer, and M.-I. Lee. 2024. "The Role of Soil Moisture-Temperature Coupling for the 2018 Northern European Heatwave in a Subseasonal Forecast." *Weather and Climate Extremes* 44: 100670.

Thompson, V., A. T. Kennedy-Asser, E. Vosper, et al. 2022. "The 2021 Western North America Heat Wave Among the Most Extreme Events Ever Recorded Globally." *Science Advances* 8: eabm6860.

Trenberth, K. E., and J. T. Fasullo. 2012. "Tracking Earth's Energy: From El Niño to Global Warming." *Surveys in Geophysics* 33: 413–426.

Wang, Q., H. Zhang, S. Yang, et al. 2022. "An Assessment of Land Energy Balance Over East Asia From Multiple Lines of Evidence and the Roles of the Tibet Plateau, Aerosols, and Clouds." *Atmospheric Chemistry and Physics* 22: 15867–15886.

Wu, B., and J. A. Francis. 2019. "Summer Arctic Cold Anomaly Dynamically Linked to East Asian Heat Waves." *Journal of Climate* 32: 1137–1150.

Yang, X., G. Zeng, S. Zhang, W. C. Wang, and V. Iyakaremye. 2021. "Cold Anomaly Over Nova Zembla–Ural Mountains: A Precursor for the Summer Long-Lived Heat Wave in Northeast Asia?" *Geophysical Research Letters* 48: e2021GL095563.

Yeh, S.-W., Y.-J. Won, J.-S. Hong, et al. 2018. "The Record-Breaking Heat Wave in 2016 Over South Korea and Its Physical Mechanism." *Monthly Weather Review* 146: 1463–1474.

Yeo, S. R., S. W. Yeh, and W. S. Lee. 2019. "Two Types of Heat Wave in Korea Associated With Atmospheric Circulation Pattern." *Journal of Geophysical Research: Atmospheres* 124: 7498–7511.

Yoon, D., D. H. Cha, G. Lee, C. Park, M. I. Lee, and K. H. Min. 2018. "Impacts of Synoptic and Local Factors on Heat Wave Events Over Southeastern Region of Korea in 2015." *Journal of Geophysical Research: Atmospheres* 123: 12,081–12,096.

Yoon, D., D.-H. Cha, M.-I. Lee, K.-H. Min, S.-Y. Jun, and Y. Choi. 2021. "Comparison of Regional Climate Model Performances for Different Types of Heat Waves Over South Korea." *Journal of Climate* 34: 2157–2174.

Yoon, D., T. Kang, D. H. Cha, et al. 2023. "Role of Land–Atmosphere Interaction in the 2016 Northeast Asia Heat Wave: Impact of Soil Moisture Initialization." *Journal of Geophysical Research: Atmospheres* 128: e2022JD037718.

Zhang, J., L. Wu, and W. Dong. 2011. "Land-Atmosphere Coupling and Summer Climate Variability Over East Asia." *Journal of Geophysical Research: Atmospheres* 116: D05117.